NYU | TANDON SCHOOL OF ENGINEERING

A Flexible Wideband Millimeter-Wave Channel Sounder with Local Area and NLOS to LOS Transition Measurements

NYU WIRELESS

IEEE International Conference on Communications (ICC)
Paris, France, May 21-25, 2017

George R. MacCartney Jr., Hangsong Yan, Shu Sun,
and Theodore S. Rappaport
{gmac,hy942,ss7152,tsr}@nyu.edu

G. R. MacCartney, Jr., H. Yan, S. Sun, and T. S. Rappaport, "A Flexible Wideband Millimeter-Wave Channel Sounder with Local Area and NLOS to LOS Transition Measurements," in 2017 IEEE International Conference on Communications (ICC) Paris, France, May 2017, pp. 1-7.

Agenda

- Background, Motivation, and Challenges
- CmWave and MmWave Channel Sounders in the Literature
- New Dual-Mode NYU Channel Sounder
- Measurement System Hardware and Calibration
- LOS to NLOS Transition and Local Area Measurements and Results
- Conclusions and Noteworthy Observations

Background

How do traditional channel sounders work at sub-6 GHz?

- TX antenna(s) with a **sectored** or is **quasi-omnidirectional** pattern
- User Equipment (UE) or RX employs **multiple omnidirectional antennas** (typically dipoles or patches)
- Multiple **RF chains** at TX and/or RX or **electronic switching** between elements
- Sophisticated post-processing algorithms to **de-embed** antenna patterns and to temporally and spatially resolve multipath components (**MPCs**): **RiMAX**; **ESPRIT**; **SAGE**; **MUSIC**
- **Less than one second to record multiple channel snapshots** (long-term synchronization not a requirement for excess delay)

Elektrobit Propsound™

Elektrobit Propsound™ Channel Sounder: IST-4-027756 WINNER II, "WINNER II channel models," European Commission, IST-WINNER, D1.1.2 V1.2, Sept. 2007. [Online]. Available: http://projects.celticinitiative.org/winner+/WINNER2-Deliverables/

Motivation

Why a new channel sounder methodology at mmWave?

- Free space path loss (FSPL) much greater in first meter of propagation:
  ~**30 dB / 36 dB more attenuation** at **30 GHz / 60 GHz** compared to **1 GHz**
- Directional horn antennas provide gain at TX/RX
- Benefits:
  1. **Increased link margin**
  2. **Spatial filtering / resolution**
  3. **Extraction of environment features** and **characteristics** for **ray-tracing** and **site-planning**
- Downsides:
  1. **0.5-4 hours for full TX/RX antenna sweeps**
  2. **Lack of synchronization** and **channel dynamics** between measurements captured at different angles
  3. **RF front-ends and components are expensive, fragile, and costly**

NYU Channel Sounder

Horn antennas

Channel Sounder Requirements

Requirements for mmWave channel modeling given new measurement methodology

- Measure path loss at long-range distances (**100's of meters**)
- Ultra-Wideband signal (**≥ 1 GHz bandwidth**) with nanosecond MPC resolution
- Angular/spatial resolution for **AOD** and **AOA modeling**
- **Real-time** measurements to capture **small-scale temporal dynamics** greater than the **Doppler rate** of the channel and **rapidly fading blockage** scenarios
- Synchronized measurements between TX and RX for **accurate time of flight / true propagation delay** and for **synthesizing omnidirectional PDPs**

Types of Channel Sounders

- Direct RF pulse systems: repetitive short probing pulse w/ envelope detection
- VNA: measures S21 parameter via IDFT
- Sliding correlator: exploits a constant envelope signal for max power efficiency; low bandwidth ADC.
- OFDM/FFT/Other types: direct-correlation / real-time with wideband ADC acquisition; thousands of PDPs/CIRs per second
- New NYU channel sounder with two modes: sliding correlator and real-time correlation (32 microsecond sampling interval). See [29] for more info.

[29] G. R. MacCartney, Jr. and T. S. Rappaport, “A flexible millimeter-wave channel sounder with absolute timing,” IEEE Journal on Selected Areas in Communications, 2017, June 2017.

Two Architectures for Channel Sounder RX

- Sliding Correlator
  - Analog correlation with RX chip rate slightly offset from TX rate: 499.9375 Mcps (slide factor of 8,000: **39 dB processing gain**)
  - Period of **time-dilated PDP** allows much **lower ADC sampling rate**:
    - $2047 \times \frac{1}{500\text{ MHz}-499.9375\text{ MHz}} = \frac{2047}{62.5\text{ kHz}} = 32.752\text{ ms}$
  - Default averaging of 20 PDPs to improve SNR: 655 ms
- Real-time spread spectrum (**direct-correlation**)
  - Sample raw I and Q baseband channels with high-speed ADC (**1.5 GS/s** on each channel): $y(t) = h(t) * x(t) \Leftrightarrow Y(f) = H(f) \cdot X(f)$
  - FFT, matched filter, and IFFT performed on periodic complex received waveform:

$$h(t) = \mathbf{IFFT}\left[\frac{\mathbf{FFT}[\boldsymbol{y}(\boldsymbol{t})]}{\mathbf{FFT}[\boldsymbol{x}(\boldsymbol{t})]}\right]$$

  - Minimum periodic PDP snapshot of 32.753 μs (30,500 PDPs per second). Memory for up to **41,000 consecutive PDPs**

[29] G. R. MacCartney, Jr. and T. S. Rappaport, “A flexible millimeter-wave channel sounder with absolute timing,” IEEE Journal on Selected Areas in Communications, June 2017.

TX Baseband Signal for Dual Mode Channel Sounder

FPGA Digital Logic and Triggers

- Variable length and repetitive **PN codes**
  - Default length: 2^{11}-1=2047 chips
  - Up to **500 Mcps** (**1 GHz RF** bandwidth)
- Extremely **long codes when memory is limited**
- Integration with **LabVIEW-FPGA** and **FlexRIO Adapter Modules** (FAM)
- DAC clocked at 125 MHz (8 ns SCTL) with 16 time-interleaved channels (**SerDes**) for **2 GS/s rates**
- **Flexible digital triggers** along chassis backplane assist **synchronization**

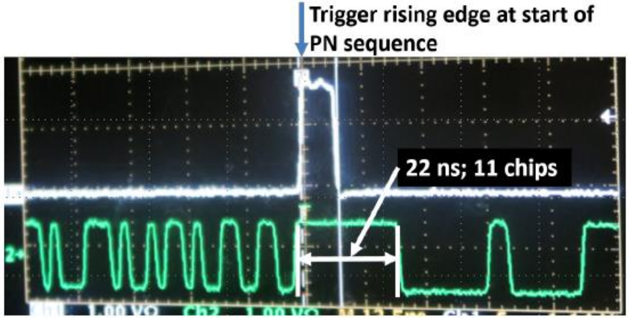

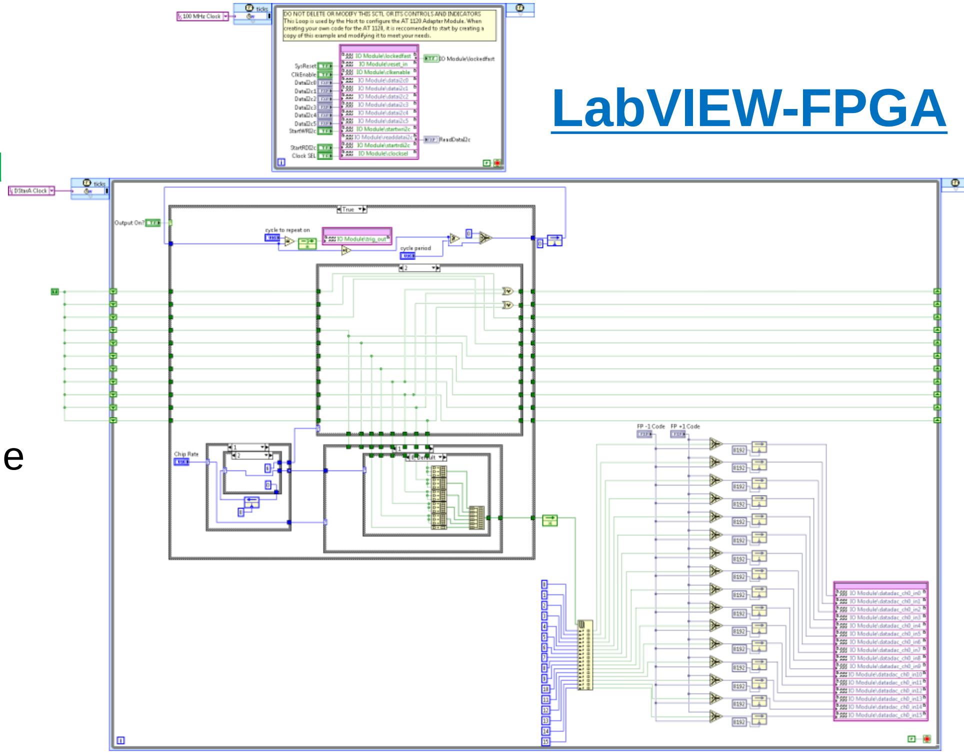

LabVIEW-FPGA

[29] G. R. MacCartney, Jr. and T. S. Rappaport, “A flexible millimeter-wave channel sounder with absolute timing,” IEEE Journal on Selected Areas in Communications, June 2017.

NYU Channel Sounder TX

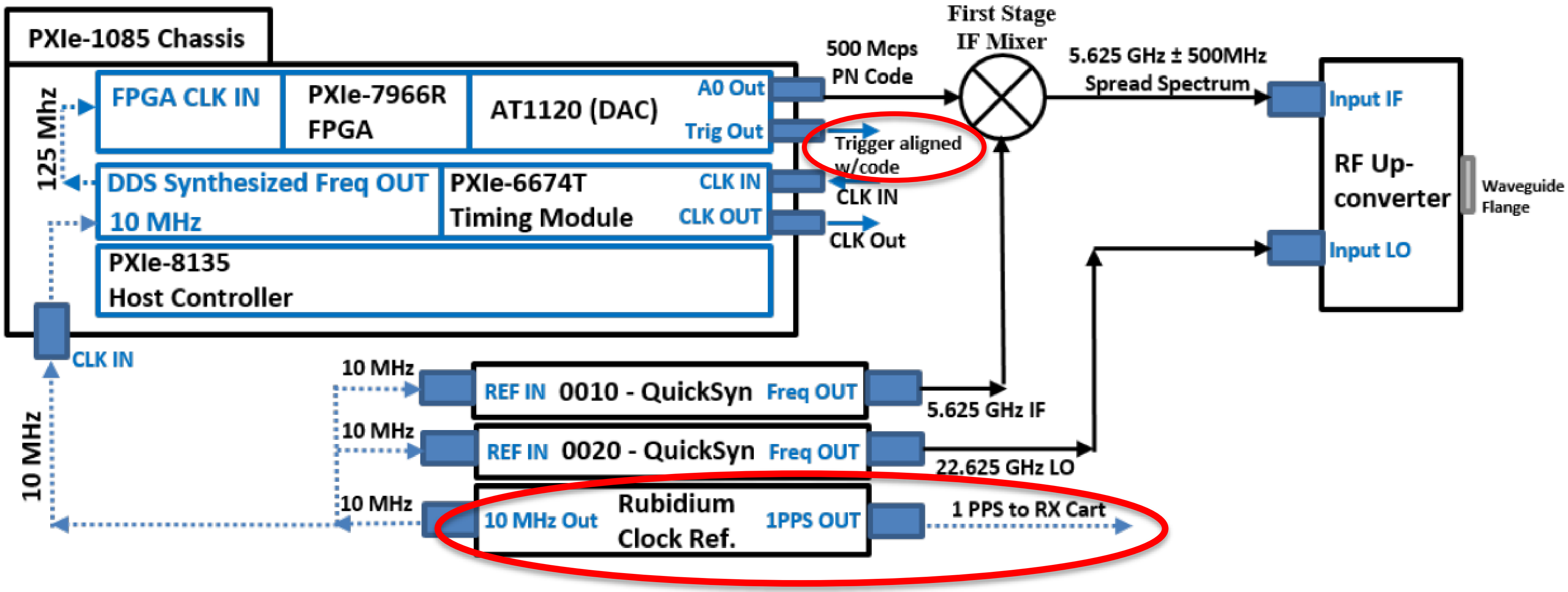

[29] G. R. MacCartney, Jr. and T. S. Rappaport, "A flexible millimeter-wave channel sounder with absolute timing," IEEE Journal on Selected Areas in Communications, June 2017.

NYU Channel Sounder RX – Sliding Correlator

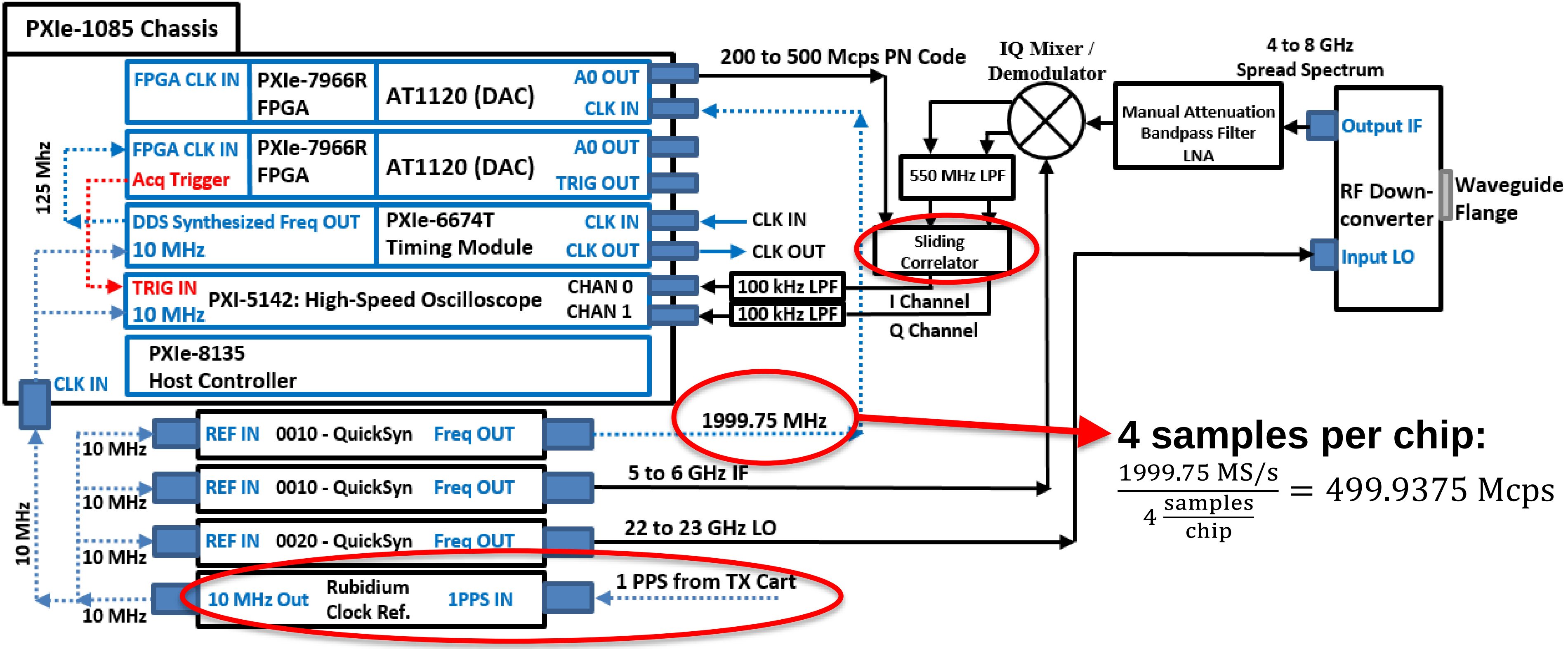

4 samples per chip:

$$\frac{1999.75\ \text{MS/s}}{4\ \frac{\text{samples}}{\text{chip}}} = 499.9375\ \text{Mcps}$$

[29] G. R. MacCartney, Jr. and T. S. Rappaport, "A flexible millimeter-wave channel sounder with absolute timing," IEEE Journal on Selected Areas in Communications, June 2017.

NYU Channel Sounder RX – Direct Correlation

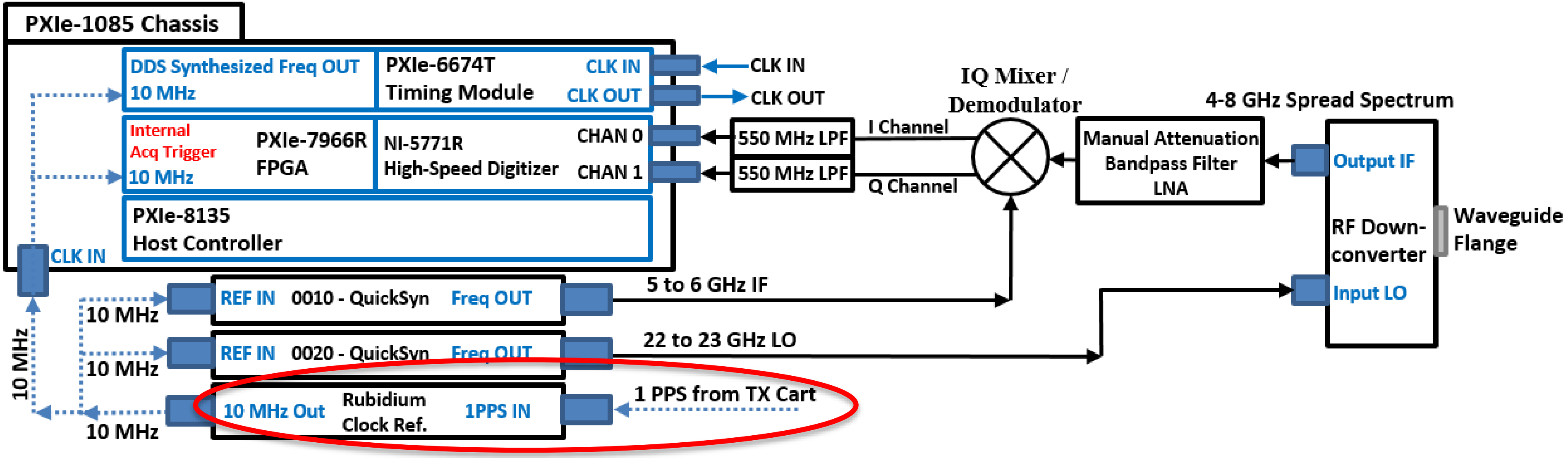

[29] G. R. MacCartney, Jr. and T. S. Rappaport, “A flexible millimeter-wave channel sounder with absolute timing,” IEEE Journal on Selected Areas in Communications, June 2017.

Antenna Control and Software Functionality

- TX/RX antenna control via FLIR Pan-Tilt D100 gimbal w/ **game controller**
- **Automatic azimuth sweeps** for AOD/AOA
- **Automatic linear track translations** for small-scale measurements
- **Real-time feedback** of channel with PDP and azimuth **power spectra display**
- Rubidium (Rb) references at TX/RX for **time/frequency synchronization**
- Ad hoc **WiFi control of TX antenna** from RX system (50 to 75m)

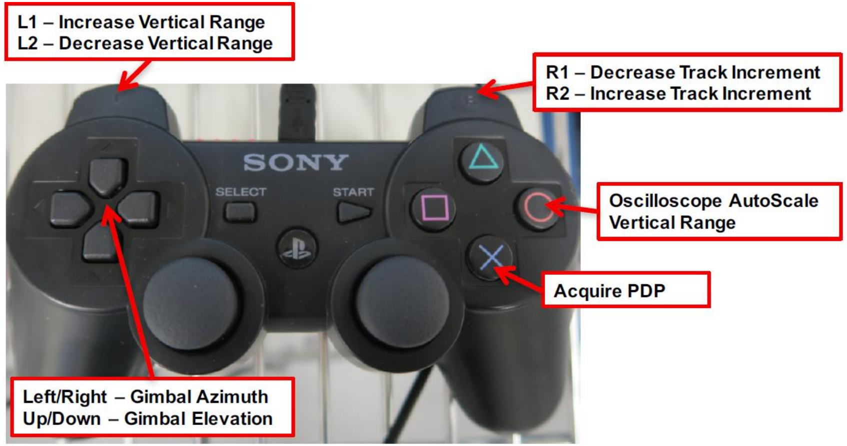

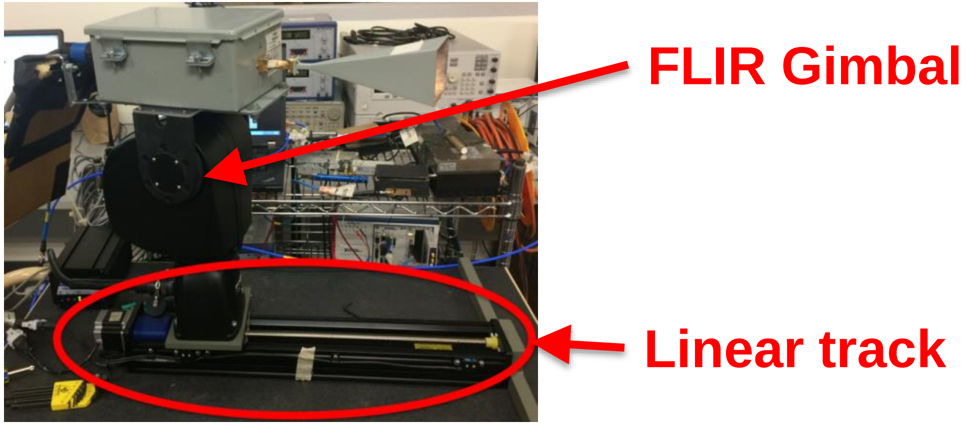

Indoor and Outdoor (Tetherless) Methods for Drift Calibration

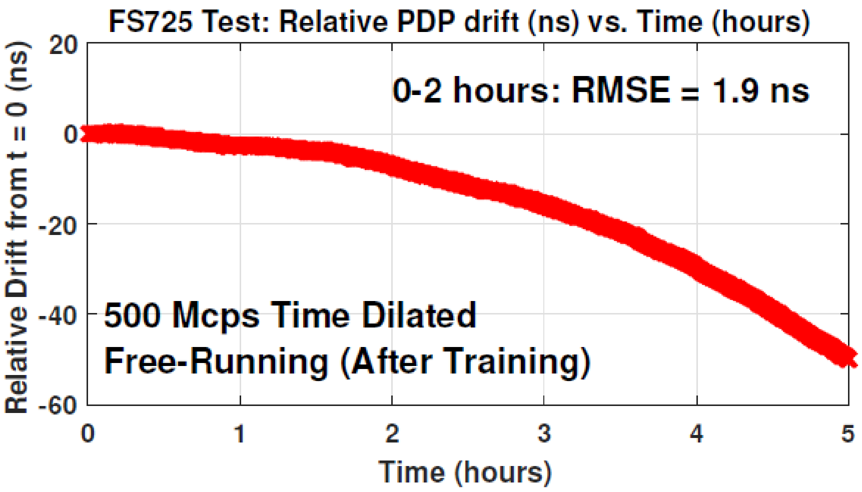

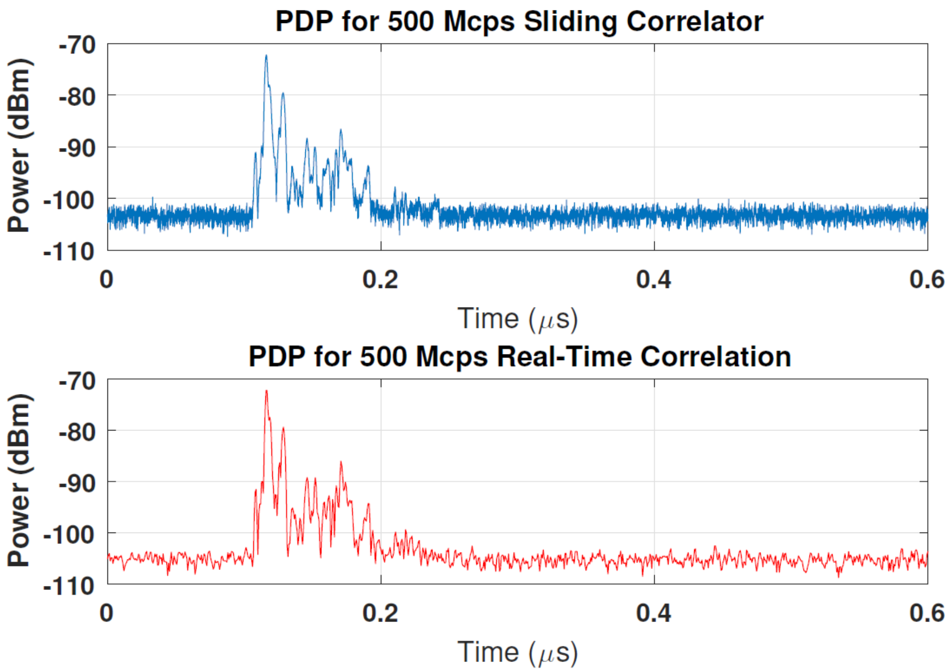

[29] G. R. MacCartney, Jr. and T. S. Rappaport, "A flexible millimeter-wave channel sounder with absolute timing," IEEE Journal on Selected Areas in Communications, June 2017.

LOS to NLOS Transition

LOS to NLOS Transition with Corner Loss in ITU-R P.1411-8

FIGURE 4

Typical trend of propagation along street canyons with low station height for frequency range from 2 to 16 GHz

Relative signal level

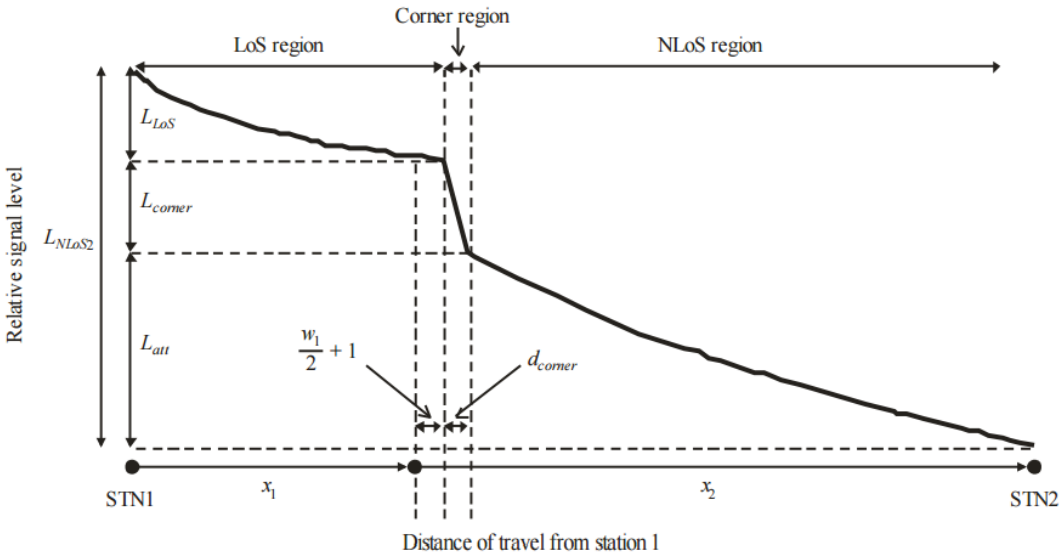

[35] International Telecommunications Union, "Propagation data and prediction methods for the planning of short-range outdoor radiocommunication systems and radio local area networks in the frequency range 300 MHz to 100 GHz," Geneva, Switzerland, Rec. ITU-R P.1411-8, July 2015.

LOS to NLOS Transition Measurements with Sliding Correlator Mode

LOS to NLOS Transition

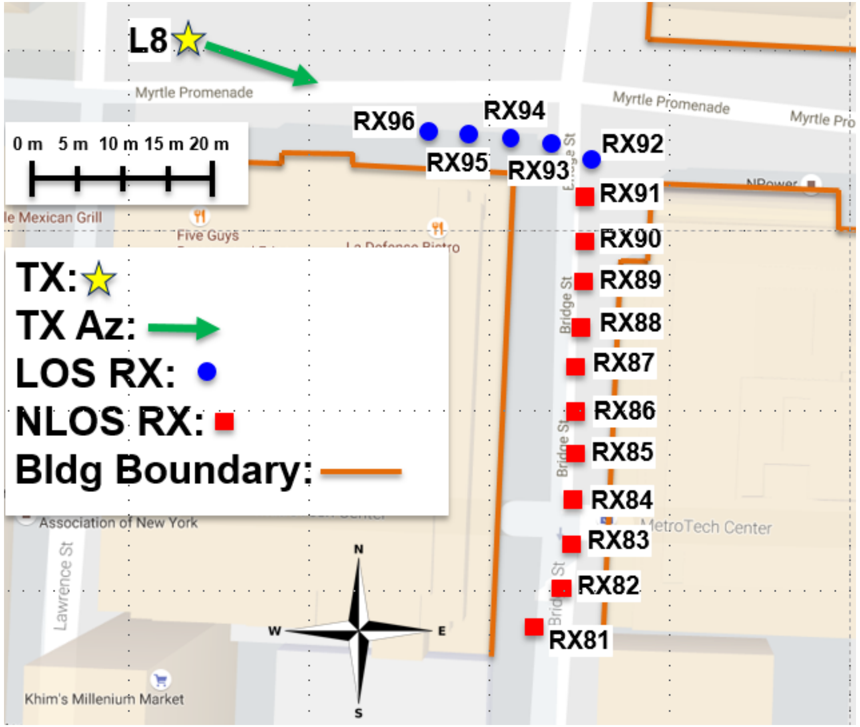

- 5 LOS: 29.6 m to 49.1 m (Euclidean)
- 11 NLOS: 50.8 m to 81.6 m (Euclidean)
- Bridge street width: 18 m
- 10 story buildings
- RX locations in **5 m adjacent** increments to form an **"L"-shaped route**
- TX antenna HPBW:7º/7º Az/El
- RX antenna HPBW:15º/15º Az/El
- TX Az/El antenna pointing angles remained fixed at 100º/0º
- RX El fixed at 0º for all locations
- RX azimuth sweeps in HPBW increments with starting position at strongest angle of arrival
- TX/RX antenna heights at 4 m / 1.5 m
- 5 repeated sweeps at each location for temporal variations

LOS to NLOS Transition Results

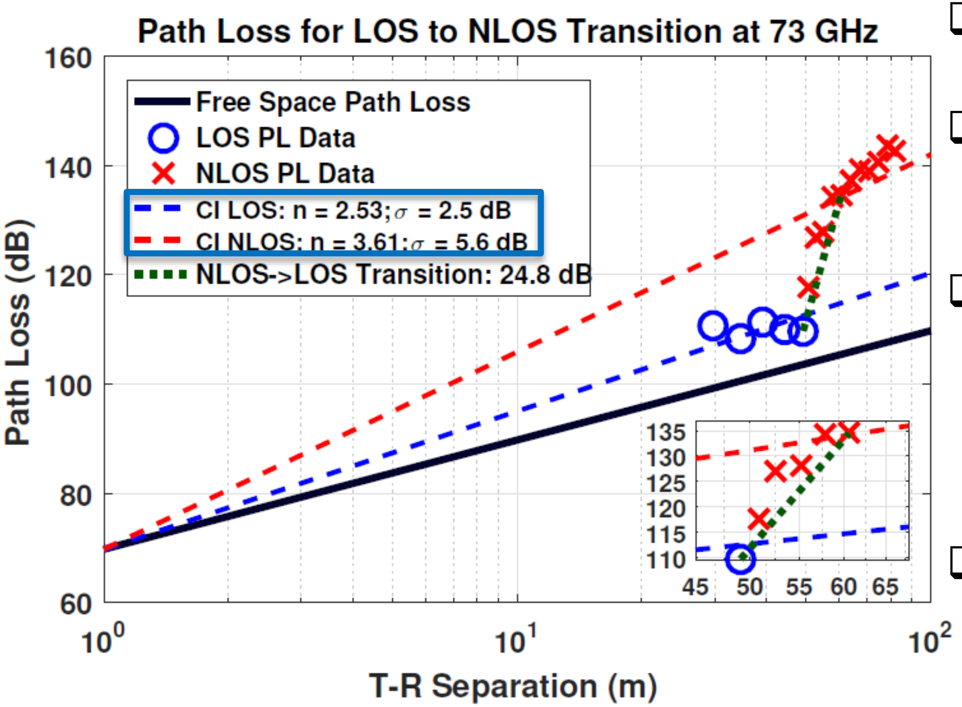

- Omnidirectional path loss synthesized from azimuth sweeps at each location [32]
- RX92 to RX87 half-way down urban canyon results in **~25 dB attenuation** (path distance of 25 meters)
- When moving around corner:
  - **Vehicle speed** of 35 m/s will experience **35 dB/s fading rate**
  - Mobile at a **walking speed** of 1 m/s will experience **1 dB/s fading rate**
- LOS PLE higher than free space due to coarse antenna boresight alignment

[32] S. Sun et al., "Synthesizing omnidirectional antenna patterns, received power and path loss from directional antennas for 5G millimeter-wave communications," in IEEE Global Communications Conference (GLOBECOM), Dec. 2015, pp. 1–7.

LOS to NLOS Transition Results

LOS

73 GHz Polar Plot at RX 92 for TX: L8

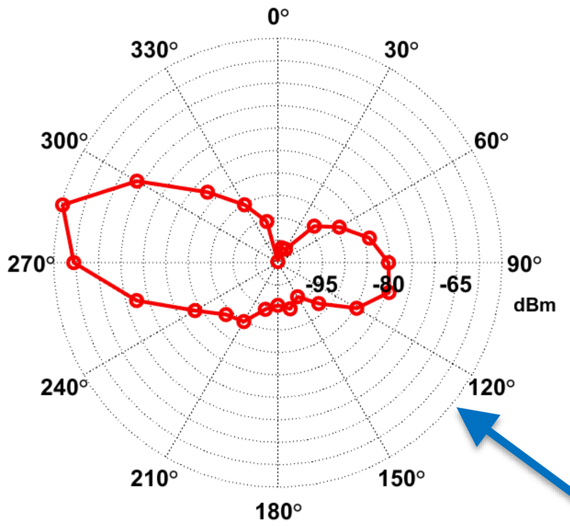

Environment: LOS

TR Separation: 49.1 m

TX Height: 4 m

RX Height: 1.5 m

Measurement: 2

$TX_{AZ/EL}$: 100°/ 0°

RX_{EL}: 0°

TX $HPBW_{AZ/EL}$: 7°/ 7°

RX $HPBW_{AZ/EL}$: 15°/ 15°

NLOS

73 GHz Polar Plot at RX 87 for TX: L8

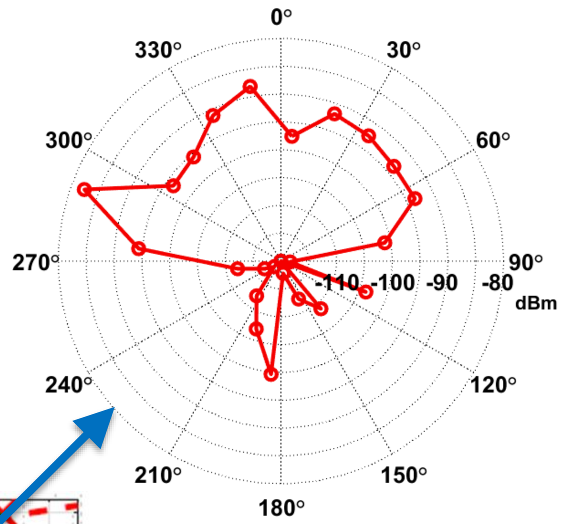

Environment: NLOS

TR Separation: 60.6 m

TX Height: 4 m

RX Height: 1.5 m

Measurement: 3

$TX_{AZ/EL}$: 100°/ 0°

RX_{EL}: 0°

TX $HPBW_{AZ/EL}$: 7°/ 7°

RX $HPBW_{AZ/EL}$: 15°/ 15°

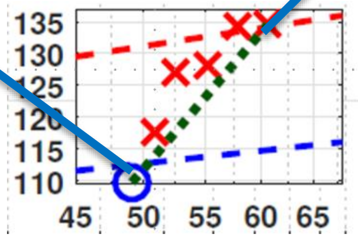

Local Area Cluster Measurements / with Sliding Correlator Mode

LOS and NLOS Local Area

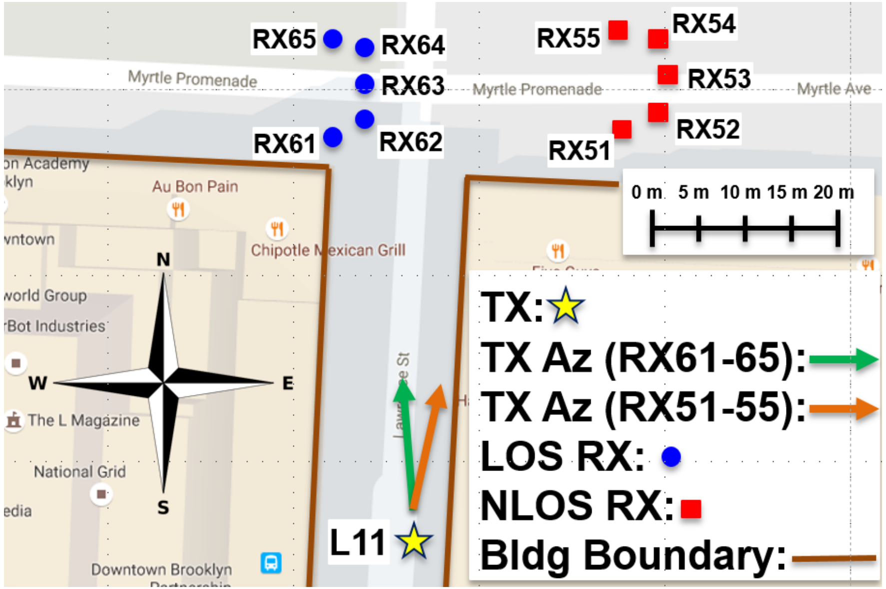

- Omnidirectional path loss synthesized from azimuth sweeps at each location [32]
- 5 LOS: 57.8 m to 70.6 m (Euclidean)
- 5 NLOS: 61.7 m to 73.7 m (Euclidean)
- RX locations for LOS and NLOS are placed in **5 m adjacent increments** that form a **semi-circle**
- **Local area grid approximately 5 m x 10 m**

Measurement Set	LOS: RX61 to RX65	NLOS: RX51 to RX55
Omnidirectional Received Power STD	4.3 dB	2.2 dB
Min/Max Omni Path Loss [dB]	105.1 dB / 114.7 dB	134.04 dB / 139.3 dB
Avg. Omni Path Loss [dB]	111 dB	137 dB

[32] S. Sun et al., "Synthesizing omnidirectional antenna patterns, received power and path loss from directional antennas for 5G millimeter-wave communications," in IEEE Global Communications Conference (GLOBECOM), Dec. 2015, pp. 1–7.

Conclusions and Observations

- New NYU dual-mode mmWave channel sounder with **sliding correlator** and **real-time spread spectrum** capabilities:
  - Long-distance (**100’s of meters**) and large-scale path loss measurements
  - Accurate **AOD and AOA angular spreads** in azimuth and elevation
  - Capture **dynamic channel fades** over short intervals in **large crowds**
- LOS to NLOS transition measurements along a route using sliding correlator
  - Results show significant **corner loss of 25 dB over a 25 m path from LOS to NLOS**
  - Two **main spatial lobes at RX in LOS** for a single TX pointing direction
- LOS and NLOS local area cluster measurements using sliding correlator
  - **Relatively low standard deviation** in received power for **LOS** RX locations in a 5 m x 10 m grid: 4.3 dB
  - **Low standard deviation** in received power for **NLOS** RX locations in a 5 x 10 m grid: 2.2 dB

NYU WIRELESS Industrial Affiliates

Acknowledgement to our NYU WIRELESS Industrial Affiliates and NSF:

NSF

at&t
CableLabs
CROWN CASTLE
ERICSSON
HUAWEI
intel
INTERDIGITAL
KEYSIGHT TECHNOLOGIES
L3 communications
NATIONAL INSTRUMENTS
nextlink
NOKIA
oppo
QUALCOMM
SiBEAM
Sprint
UMC
verizon

References

[1] Z. Pi and F. Khan, “An introduction to millimeter-wave mobile broadband systems,” IEEE Communications Magazine, vol. 49, no. 6, pp. 101–107, June 2011.
[2] F. Boccardi et al., “Five disruptive technology directions for 5G,” IEEE Communications Magazine, vol. 52, no. 2, pp. 74–80, Feb. 2014.
[3] T. S. Rappaport, W. Roh, and K. Cheun, “Mobile’s millimeter-wave makeover,” in IEEE Spectrum, vol. 51, no. 9, Sept. 2014, pp. 34–58.
[4] Federal Communications Commission, “Spectrum Frontiers R&O and FNPRM: FCC16-89,” July. 2016. [Online]. Available: https://apps.fcc.gov/edocs public/attachmatch/FCC-16-89A1 Rcd.pdf
[5] 3GPP, “Technical specification group radio access network; channel model for frequency spectrum above 6 GHz (Release 14),” 3rd Generation Partnership Project (3GPP), TR 38.900 V14.2.0, Dec. 2016. [Online]. Available: http://www.3gpp.org/DynaReport/38900.htm
[6] W. G. Newhall, T. S. Rappaport, and D. G. Sweeney, “A spread spectrum sliding correlator system for propagation measurements,” in RF Design, Apr. 1996, pp. 40–54.
[7] W. G. Newhall, K. Saldanha, and T. S. Rappaport, “Using RF channel sounding measurements to determine delay spread and path loss,” in RF Design, Jan. 1996, pp. 82–88.
[8] W. G. Newhall and T. S. Rappaport, “An antenna pattern measurement technique using wideband channel profiles to resolve multipath signal components,” in Antenna Measurement Techniques Association 19th Annual Meeting & Symposium, Nov. 1997, pp. 17–21.
[9] Aalto University, AT&T, BUPT, CMCC, Ericsson, Huawei, Intel, KT Corporation, Nokia, NTT DOCOMO, New York University, Qualcomm, Samsung, University of Bristol, and University of Southern California, “5G channel model for bands up to 100 GHz,” 2016, Oct. 21. [Online]. Available: http://www.5gworkshops.com/5GCM.html
[10] K. Haneda et al., “5G 3GPP-like channel models for outdoor urban microcellular and macrocellular environments,” in 2016 IEEE 83rd Vehicular Technology Conference (VTC2016-Spring), May 2016, pp. 1–7.
[11]] K. Haneda et al., “Indoor 5G 3GPP-like channel models for office and shopping mall environments,” in 2016 IEEE International Conference on Communications Workshops (ICCW), May 2016, pp. 694–699.
[12] S. Sun et al., “Investigation of prediction accuracy, sensitivity, and parameter stability of large-scale propagation path loss models for 5G wireless communications (Invited Paper),” IEEE Transactions on Vehicular Technology, vol. 65, no. 5, pp. 2843–2860, May 2016.
[13] G. R. MacCartney, Jr. et al., “Indoor office wideband millimeter-wave propagation measurements and models at 28 GHz and 73 GHz for ultradense 5G wireless networks (Invited Paper),” IEEE Access, pp. 2388–2424, Oct. 2015.
[14] T. S. Rappaport et al., “Wideband millimeter-wave propagation measurements and channel models for future wireless communication system design (Invited Paper),” IEEE Transactions on Communications, vol. 63, no. 9, pp. 3029–3056, Sept. 2015.

References

[15] IST-4-027756 WINNER II, “WINNER II channel models,” European Commission, IST-WINNER, D1.1.2 V1.2, Sept. 2007. [Online]. Available: http://projects.celticinitiative.org/winner+/WINNER2-Deliverables/
[16] 3GPP, “Technical specification group radio access network; study on 3D channel model for LTE (Release 12),” 3rd Generation Partnership Project (3GPP), TR 36.873 V12.2.0, June 2015. [Online]. Available: http://www.3gpp.org/dynareport/36873.htm
[17] B. Thoma, T. S. Rappaport, and M. D. Kietz, “Simulation of bit error performance and outage probability of /4 DQPSK in frequency-selective indoor radio channels using a measurement-based channel model,” in IEEE Global Telecommunications Conference (GLOBECOM). Communication for Global Users, vol. 3, Dec 1992, pp. 1825–1829.
[18] T. S. Rappaport, Wireless Communications: Principles and Practice, 2nd ed. Upper Saddle River, NJ: Prentice Hall, 2002, ch. 4, 5.
[19] P. B. Papazian et al., “A radio channel sounder for mobile millimeter-wave communications: System implementation and measurement assessment,” IEEE Transactions on Microwave Theory and Techniques, vol. 64, no. 9, pp. 2924–2932, Sept. 2016.
[20] S. Salous et al., “Wideband MIMO channel sounder for radio measurements in the 60 GHz band,” IEEE Transactions on Wireless Communications, vol. 15, no. 4, pp. 2825–2832, Apr. 2016.
[21] Z. Wen et al., “mmWave channel sounder based on COTS instruments for 5G and indoor channel measurement,” in 2016 IEEE Wireless Communications and Networking Conference, Apr. 2016, pp. 1–7.
[22] J. J. Park et al., “Millimeter-wave channel model parameters for urban microcellular environment based on 28 and 38 GHz measurements,” in 2016 IEEE 27th Annual International Symposium on Personal, Indoor, and Mobile Radio Communications (PIMRC), Sept. 2016, pp. 1–5.
[23] E. Ben-Dor et al., “Millimeter-wave 60 GHz outdoor and vehicle AOA propagation measurements using a broadband channel sounder,” in 2011 IEEE Global Telecommunications Conference (GLOBECOM), Dec. 2011, pp. 1–6.
[24] D. Cox, “Delay doppler characteristics of multipath propagation at 910 MHz in a suburban mobile radio environment,” IEEE Transactions on Antennas and Propagation, vol. 20, no. 5, pp. 625–635, Sept. 1972.
[25] C. Chu, P. P. Chu, and R. E. Jones, “Design techniques of FPGA based random number generator,” in Military and Aerospace Applications of Programmable Devices and Technology Conference. Hopkins University Applied Physics Laboratory, Sept. 1999.
[26] T. S. Rappaport et al., “Millimeter Wave Mobile Communications for 5G Cellular: It Will Work!” IEEE Access, vol. 1, pp. 335–349, May 2013.
[27] S. Nie et al., “72 GHz millimeter wave indoor measurements for wireless and backhaul communications,” in 2013 IEEE 24th International Symposium on Personal Indoor and Mobile Radio Communications (PIMRC), Sept. 2013, pp. 2429–2433.
[28] G. R. MacCartney, Jr. and T. S. Rappaport, “73 GHz millimeter wave propagation measurements for outdoor urban mobile and backhaul communications in New York City,” in 2014 IEEE International Conference on Communications (ICC), June 2014, pp. 4862–4867.

References

[29] G. R. MacCartney, Jr. and T. S. Rappaport, "A flexible millimeter-wave channel sounder with absolute timing," IEEE Journal on Selected Areas in Communications, June 2017.
[30] M. I. Skolnik, Introduction to Radar Systems, 3rd ed. New York, NY, USA: McGRAW-HILL, 2001.
[31] G. R. MacCartney, Jr., M. K. Samimi, and T. S. Rappaport, "Omnidirectional path loss models in New York City at 28 GHz and 73 GHz," in IEEE 25th International Symposium on Personal Indoor and Mobile Radio Communications (PIMRC), Sept. 2014, pp. 227–331.
[32] S. Sun et al., "Synthesizing omnidirectional antenna patterns, received power and path loss from directional antennas for 5G millimeter-wave communications," in IEEE Global Communications Conference (GLOBECOM), Dec. 2015, pp. 1–7.
[33] M. K. Samimi et al., "28 GHz angle of arrival and angle of departure analysis for outdoor cellular communications using steerable beam antennas in New York City," in 2013 IEEE 77th Vehicular Technology Conference (VTC-Spring), June 2013, pp. 1–6.
[34] S. Sun et al., "Millimeter wave small-scale spatial statistics in an urban microcell scenario," in 2017 IEEE International Conference on Communications (ICC), May 2017, pp. 1–7.
[35] International Telecommunications Union, "Propagation data and prediction methods for the planning of short-range outdoor radiocommunication systems and radio local area networks in the frequency range 300 MHz to 100 GHz," Geneva, Switzerland, Rec. ITU-R P.1411-8, July 2015.

Thank You!

Questions